Cell Biochem Biophys (2016) 74:337–351
DOI 10.1007/s12013-016-0741-x

ORIGINAL PAPER

Ethyl 4-(4-methylphenyl)-4-pentenoate from *Vetiveria zizanioides* Inhibits Dengue NS2B–NS3 Protease and Prevents Viral Assembly: A Computational Molecular Dynamics and Docking Study

P. Lavanya[1] · Sudha Ramaiah[1] · Anand Anbarasu[1]

Received: 25 June 2014 / Accepted: 9 June 2016 / Published online: 21 June 2016

Abstract Around 50 % of the world's population is at the risk of dengue, a viral infection. Presently, there are not many drugs and prophylactic measures available to control dengue viral infection, and hence, there is an urgent need to develop effective antidengue compound from natural sources. In the current study, we explored the antiviral properties of the medicinal plant *Vetiveria zizanioides* against dengue virus. Initially, the antiviral properties of active compounds were examined using docking analysis along with reference ligand. The enzyme–ligand complex which showed higher binding affinity than the reference ligand was employed for subsequent analysis. The stability of the top scoring enzyme–ligand complex was further validated using molecular simulation studies. On the whole, the study reveals that the compound Ethyl 4-(4-methylphenyl)-4-pentenoate has an effective antiviral property, which can serve as a potential lead molecule in drug discovery process.

Keywords Dengue virus · NS2B–NS3 protease · *Vetiveria zizanioides* · ADMET · Molecular dynamics

Abbreviations

ADMET	Absorption, distribution, metabolism, excretion, and toxicity
CDC	Centre for Disease Control and Prevention
DENV	Dengue virus
LINCS	Linear constraint solver
MOLCAD	Molecular computer-aided design
NS	Nonstructural
NVT	Constant number of particles, volume, and temperature
NPT	Constant number of particles, pressure, and temperature
PDB	Protein data bank
PME	Particle mesh Ewald
RMSD	Root mean square deviation
RMSF	Rood mean square fluctuation
Vetiveria zizanioides	*V. zizanioides*

✉ Anand Anbarasu
aanand@vit.ac.in

[1] Medical & Biological Computing Laboratory, School of Biosciences and Technology, VIT University, Vellore 632014, Tamil Nadu, India

Introduction

Dengue viral infection is emerging as a major health concern throughout the world. Dengue was ranked as the most important arthropod-borne viral infection in 2012. As reported by US Centre for Disease Control and Prevention (CDC) around 2.5 billion people are at the risk of dengue infection Hynes [1]. The severity of dengue can lead to lethal conditions such as dengue hemorrhagic fever and dengue shock syndrome [2]. Despite the importance, there is no effective vaccine available to combat the severity of dengue viral infection [3]. Dengue virus has a single-stranded RNA genome and it belongs to the family *Flaviviridae* [4]. Dengue viruses are classified into four types based on the antigenic differences on the envelope protein [5]. Proteolysis of the dengue virus genome yields three structural and seven nonstructural proteins [6]. During viral maturation, the polyprotein is cleaved by the NS3 serine protease at the N-terminal domain, interceded by the cofactor NS2B [7]. Processing

of this polyprotein is a fundamental process that must occur before viral RNA replication process. NS3 is a multifunctional protein of 618 amino acids that function as serine protease as well as an RNA helicase. Protease domain is N-terminal in NS3 and cleaves the viral polyprotein at several sites [8]. This enzyme consists of 6 β-strands that form two β-barrels with the catalytic triad (His-51, Asp-75, Ser-135) arranged between them. Activity of protease is crucially dependent upon the presence of its cofactor, NS2B which is a conserved region among the flaviviruses. The NS3 protein included residues 49–66 from the NS2B which were linked to the N-terminus of full-length Ns3 by Gly-Ser linker. The cis/trans-activity of many flavivirus proteases is proved to play an important role in controlling dynamics of viral protein translation and also the replication process by controlling the availability of viral proteins [9, 10]. NS3 protease is the primary target for the development of effective antiviral drugs, since the enzyme plays an important role in the replication process [11].

Medicinal plants are important sources of drug discovery because of their minimal side effects and high efficiency. Around 25 % of the drugs which are currently used to treat a wide variety of health complications are of plant origin [12]. With the advancement in silico methodologies, medicinal plants have become a new source of drug discovery process. World Health Organization estimates that 80 % of people in developing countries rely on traditional herbal medicines [13]. *Vetiveria zizanioides* is a medicinal plant and it is known to possess several biological activities such as antioxidant, antibacterial, antifungal, and antitubercular properties [14]. Active compounds present in the leaves of *V. zizanioides* are also widely used in the treatment of rheumatism [15]. The oil obtained from *V. zizanioides* contains a complex mixture of sesquiterpene alcohols and hydrocarbons. In India *V. zizanioides* is used for the treatment of numerous conditions like gastritis, fever, and other inflammatory conditions [16]. Chemical examination of vetiver oil from *V. zizanioides* has been the subject of investigation for its pharmacological and biological activities by many workers [17]. Literature analysis reveals that only a few scientific studies have been undertaken to evaluate the antiviral property of *V. zizanioides*. Therefore, the present study aims at exploring the antiviral activities of *V. zizanioides* and providing scientific evidence for its use as an effective antiviral medicine. Many viruses depend on polymerases, proteases, and other vital enzymes for their survival and proliferation. Inhibition of these key enzymes offers a promising strategy to develop an effective antiviral inhibitor. Hence, we carried out this research to explore the antiviral properties of *V. zizanioides* against dengue virus protease by in silico approaches. Our results will be a good starting point for experimental biologists exploring plant-based antidengue compounds.

Materials and Methods

Choosing Protein Structure

The three-dimensional structures of dengue virus protease were retrieved from protein data bank (PDB) [18]. The PDB structures employed for the present study are listed below:

i. DENV-1 protease—3L6P [19],
ii. DENV-2 protease—2FOM [20],
iii. DENV-3 protease—3U1J [21], and
iv. DENV-4 protease—2WHX [22].

Collection of Active Compounds

The three-dimensional structures of active compounds from *V. zizanioides* were collected from PubChem database based on literature studies [23]. Panduratin, a biologically active compound from *Boesenbergia rotunda*, was used as a reference ligand [24].

Molecular Docking Studies

Docking analysis was performed with Surflex-dock program incorporated in SYBYL 2.0 [25]. Surflex dock effectively screens the active compounds by combining Hammerhead docking scoring function with the search engine, which generates putative poses for molecular splinters. The binding affinity between the ligand and the target was calculated using empirically derived scoring functions. In Surflex dock, consensus scoring function was used to evaluate the binding affinity between the ligand and receptor. Cscore effectively removed the false-positive results by combining multiple scoring functions. Cscore is a combination of Gold score (Gscore), Dock score (Dscore), potential mean force score (PMF score), polar score, and crash score. Gscore calculates the energetic contribution from hydrogen bond interactions [26], Dscore calculates the energetic contribution from hydrophobic and electrostatic interactions [27], and Chemscore calculates the energetic contribution from lipophilic and hydrogen bonding interactions [28]. Before docking, the structure of protein should be optimized by the addition of hydrogen atoms; the cocrystallized and other unrelated structures should be removed. Finally, the structure undergoes a brief energy minimization using the force field AMBER 7 FF99. Molecular computer-aided

design (MOLCAD), a visualization tool, was used to observe the interaction between ligand and the receptor.

Molecular Dynamics and Simulation

Estimating the binding affinity of small molecules is a key process in designing effective drugs [29]. The molecular dynamics simulation of the dengue virus protease with respect to the reference and active ligands was performed for a period of 20 ns using Gromacs 4.5.5 [30]. Initially, the complex was solvated using simple point charge (SPC) water molecules [31]. The force field used for the simulation of protein–ligand complex was Gromacs96 43a1. In order to neutralize the protein which was positively charged, counter ions (Cl− or Na+) were added using the genion program of the gromacs simulation suite. To remove the van der Waals short contacts, all hydrogen atoms, ions, and water molecules were subjected to 1000 steps of energy minimization by the steepest descent method. The system was then subjected to two phases of equilibration for a period of 1000 ps. The first phase included NVT ensemble in which endothermic and exothermic processes were exchanged with the thermostat. The second phase contained NPT ensemble at 300 k along with constant pressure. The LINCS (linear constraint solver) algorithm with a 10^{-4} Å tolerance was applied to constrain all the covalent bonds. The electrostatic interactions were evaluated using Particle Mesh Ewald (PME) method within a charge grid space of 0.30 Å. The Lennard-Jones interactions were analyzed using a 9.0 Å atom-based cut-off. Finally, MD was performed for a period of 20 ns to analyze the stability of each system. Further, the free energies of binding for the Ethyl 4-(4-methylphenyl)-4-pentenoate–DENV-4 complex and panduratin–DENV-4 complex were analyzed using normal mode analyses using the program Elnemo [32]. Gromacs package was used to minimize the structure of Ethyl 4-(4-methylphenyl)-4-pentenoate–DENV-4 complex and panduratin–DENV-4 complex. 1000 steps of steepest descent energy minimization were carried out for the enzymes. The collective motion in the energy minimized structure was generated by means of normal mode analysis. We have chosen the seventh mode for the study as most of the protein movements can be modeled by using low-frequency normal modes. The normal mode analysis generates 11 possible confirmations between DQMIN of 100 and DQMAX of 100 with DQSTEP size of 20 [32].

Trajectory Analysis

The convergence of simulation was analyzed in terms of total energy, root mean square deviation (RMSD), root mean square fluctuation (RMSF), and the number of H bonds formed between the ligand and receptor using the Gromacs utilities [33].

Calculation of Drug-likeness and Molecular Properties of Active Compounds

Molecular properties of the active compound which showed maximum binding affinity with the dengue virus were analyzed using the server Molinspiration (http://www.molinspiration.com/) and ADMET properties were calculated using the tool admetSAR [34]. ADMET profiling include parameters such as blood–brain barrier (BBB), Human intestinal absorption (HIA), Caco-2 permeability, p-glycoprotein inhibitor, Renal organic cation transporter, CYP450 (Cytochrome P450) 2C9 Substrate, CYP450 2D6 Substrate, CYP450 3A4 Substrate, CYP450 1A2 Inhibitor, CYP450 2C9 Inhibitor, CYP450 2D6 Inhibitor, CYP450 2C19 Inhibitor, CYP450 3A4 Inhibitor, and AMES Toxicity.

Results and Discussion

Dengue virus disease is becoming a serious health threat worldwide [35] and there is an urgent need to develop potential antidengue compounds to combat dengue virus. Hence, in the present study, we employed various computational techniques to identify a potential plant-based antidengue compound. During the past decade, several computational strategies have been developed to analyze the resistance mechanism produced by the alteration in the binding site of the target [36]. Drug resistance can be divided into several categories including target mutation and epigenetic modifications characterized by gene expression variations of the target protein [37]. Thus, it is obligatory to computationally predict the possible mutation-induced drug resistance and to design possible inhibitors that are also effective against the resistant variants. In general, molecular docking [38], molecular dynamics [39], and computational mutation scanning methods [40] have been used to determine the binding structures of a drug in various mutants. Because of the high efficiency of the computation, molecular docking analysis is a valuable option for the resistance prediction of a large number of mutants or compounds. Further molecular simulation has an advantage in conformational flexibility sampling and atom-level motion can be obtained from trajectories. Hence, the antiviral properties of active compounds were examined using docking analysis and the conformational stability of the enzyme–ligand complex is further validated using molecular simulation analysis. Finally, the ADMET property of the active compound is analyzed to check the capability of compound to act as an efficient drug candidate.

Molecular Docking Studies

Increase in the global spread of dengue virus and the lack of an approved vaccine prompted us to carry out this work. Dengue virus infection is caused by four closely related serotypes namely DENV-1, DENV-2, DENV-3, and DENV-4. Even though these viruses show 65 % of similarity in their genome, these serotypes shows difference in the type of interactions with the antiviral drugs. Hence in the present study, we explored the antiviral properties of active compounds from *Vetiveria zizanioides* against all the four types of dengue virus protease. The active site residues present in the protease of all four dengue virus are identified to generate protomol. For better understanding, the active site residues of all the four types of proteases are listed in revised Table 1. In addition, figures illustrating the active site residues of all the types of proteases are illustrated in revised Fig. 1. The aim of our study is to identify novel dengue virus protease inhibitors for the development of effective antidengue compounds from plant sources. NS2B–NS3 protease acts as a promising target for the antiviral drugs since it plays an important role in viral replication process [41, 42]. In the present study, docking analysis was performed on a series of active compounds against the NS2B–NS3 protease that play a crucial role in dengue virus replication [43]. In order to identify the efficiency of active compounds, our results were also compared with the reference ligand panduratin [24]. The binding affinity of active compounds from *V. zizanioides* with the DENV-1 protease is shown in revised Table 2. Our analysis revealed that the compound Ethyl 4-(4-methylphenyl)-4-pentenoate showed maximum binding affinity with DENV-1 protease comparing to the rest of the compounds analyzed. Even though Cedr-8-en-13-o1 showed the highest score similar to Ethyl 4-(4-methylphenyl)-4-pentenoate, the energetic contribution from protein–ligand atom pair interaction was comparatively less. The reference ligand panduratin which demonstrated the next highest score showed poor values in all the parameters except Helmholtz free energies. Sativan, a flavonoid which is proven to be effective against mycobacterium tuberculosis, showed the least score among the 25 compounds examined. It was also interesting to find that the compounds 2,3,5,5,8,8-Hexamethyl-cycloocta-1,3,6-triene, β-Guaiene, Widdrol, α-Amorphene, α-Gurjunene Ledene, Epiglobulol, 6-Isopropenyl-4,8 a-dimethyl-1,2,3,5,6,7,8,8a-Octahydro-naphthalen-2-ol, and 3,8-Dimethyl-4-(1-methylethylidene)-2,4,6,7,8,8a-Hexahydro-5(1H)-azulenone exhibited scores in the similar range but the consensus score was comparatively lesser than that of Ethyl 4-(4-methylphenyl)-4-pentenoate. Revised Table 3 shows the energy of binding affinity of active compounds towards the protease of DENV-2 virus. It is worth mentioning that similar to DENV-1 results, the compound Ethyl 4-(4-methylphenyl)-4-pentenoate ranked the highest among the active compounds analyzed. Epiglobulol, the compound with antiviral activity scored the next highest score but showed poor values in terms of energetic contribution from van der Waals interactions. Considering the compound 3,3,8,8-Tetramethyl-tricyclo[5.1.0.0(2,4)] oct-5-ene-5-propanoic acid, and 3,8-Dimethyl-4-(1-methylethylidene)-2,4,6,7,8,8a-Hexahydro-5(1H)-azulenone, which showed the considerable binding affinity between the ligand and the receptor, we observed that it had the least value in the potential of mean force (PMF) score. The reference ligand panduratin and the active compound α-Amorphene showed similar binding affinity with the DENV-2 protease, but the energetic contribution from hydrogen bonding, protein–ligand atom pair complex was comparatively lesser than that of the active compound Ethyl 4-(4-methylphenyl)-4-pentenoate. Results of the binding pattern of DENV-3 virus are depicted in revised Table 4. It is interesting to find that the compound Ethyl 4-(4-methylphenyl)-4-pentenoate exhibited higher value compared to all the active compounds analyzed. Similar to DENV-2 results, the compound Epiglobulol showed the second highest value after Ethyl 4-(4-methylphenyl)-4-pentenoate which has been previously reported to possess antiseptic activity and antibacterial activity. The next highest binding affinity was shown by the compound 6-Isopropenyl-4, 8 a-dimethyl-1,2,3,5,6,7,8,8a-Octahydro-naphthalen-2-ol, but the total score was lesser than that of the reference ligand. The

Table 1 Active site residues present in the protease of dengue virus serotypes

Dengue virus serotypes	Active site residues
DENV-1	Met 99, Lys 123, Lys 124, Asp 125, Phe 166, Thr 168, Gly 171, Val 173, Ala 175, Gly 201, Asn 202, Gly 203, Val 204, Val 212, Ala 214, Ile 215, Ala 216, Gln 217
DENV-2	Glu 52, Leu 53, Glu 54, His 60, Lys 61, Leu 95, Gly 96, Lys 87, Glu 90, Glu 91, Thr 94, Gly 96
DENV-3	Ile 19, Gln 27, Lys 42, Ala 57, Asp 58, Thr 60, Glu 62, Leu 85, Ser 86, Gln 88, Trp 89, Gln 90, Glu 93, Gly 144
DENV-4	Thr 200, Lys 201, Pro 223, Thr 224, Arg 225, Val 226, Tyr 242, Pro 245, Cys 261, His 262, Ala 263, Thr 264, Leu 270, His 287, Phe 288, Thr 289, Asp 290, Pro 291, Cys 292, Ser 293, Arg 317, Gly 320, Thr 322, Ile 365, Arg 387, Asp 391, Thr 408, Ile 410

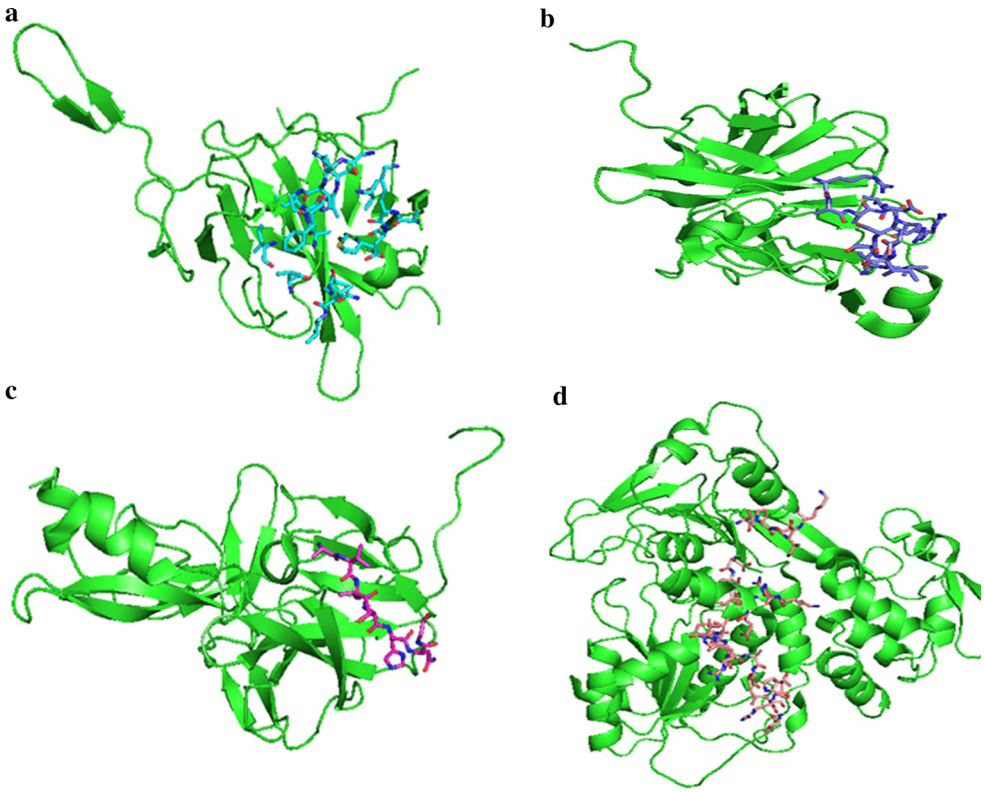

Fig. 1 Active site residues present in the protease of dengue virus. **a** DENV-1, **b** DENV-2, **c** DENV-3, **d** DENV-4

reference ligand panduratin which had a total score similar to the compound Epiglobulol showed poor values in hydrogen bonding parameters. Considering the energetic contribution from hydrogen bonding and ligand–protein complex, the compound Cedr-8-en-13-ol scored the best. The compound Sativan showed the least binding affinity among the compounds analyzed; the result was similar to DENV-1 protease. Other compounds such as Spathulenol, Isovellerdiol, Cubenol, Dehydro-aromadendrene, and 2-Isopropenyl-1,3,5-trimethylbenzene showed lesser values than Ethyl 4-(4-methylphenyl)-4-pentenoate and reference ligand. The binding affinity of the active compounds with DENV-4 is depicted in revised Table 5. It is interestingly observed that the compound Ethyl 4-(4-methylphenyl)-4-pentenoate demonstrated the highest consensus score with DENV-4 protease. Even though Ethyl 4-(4-methylphenyl)-4-pentenoate showed highest binding affinity with DENV-1, DENV-2, and DENV-3 serotypes, the total score obtained was comparatively higher than the other serotypes. Pictorial representation of hydrogen bond interaction between the DENV-4 protease and active compound is shown in revised Fig. 2. The reference ligand panduratin which showed maximum binding next to the top ranked ligand was also found to be effective but the number of hydrogen bond formed was relatively lesser than the top ranked ligand, as shown in revised Fig. 3. On the whole, from the docking analysis we could conclude that the compound Ethyl 4-(4-methylphenyl)-4-pentenoate showed maximum binding affinity with all the serotypes analyzed and the highest binding interaction was observed between DENV-4 protease–Ethyl 4-(4-methylphenyl)-4-pentenoate complex. The free energy binding of DENV-4 protease with Ethyl 4-(4-methylphenyl)-4-pentenoate and panduratin is shown in revised Table 6. We observed that free energy of binding for Ethyl 4-(4-methylphenyl)-4-pentenoate–DENV-4 complex is substantially higher than panduratin–DENV-4 complex in all the conformations analyzed. These observations confirmed the antiviral property of Ethyl 4-(4-methylphenyl)-4-pentenoate against DENV-4.

Molecular Dynamics of the Complexes

Molecular dynamic studies provide insight into conformational changes induced by the binding of active compound Ethyl 4-(4-methylphenyl)-4-pentenoate with dengue virus protease. The equilibration and the stability pattern of high scored Ethyl 4-(4-methylphenyl)-4-pentenoate is compared with reference ligand panduratin in terms of potential energy of the system, RMSD, hydrogen bonds, and RMSF analysis. Our MD results reveal that the DENV-4 protease–Ethyl 4-(4-methylphenyl)-4-pentenoate complex is stable as indicated by the results provided below.

Table 2 Binding affinity of active compounds with NS2B–NS3 protease of DENV-1 virus

S.No	Compounds	Cscore[a]	Crash score[b]	Polar score[c]	Dscore[d]	PMF score[e]	Gscore[f]	Chem score[g]
1	Ethyl 4-(4-methylphenyl)-4-pentenoate	4.39	0.56	2.07	−77.9	−19.5	−117.3	−20
2	2,3,5,5,8,8-Hexamethyl-cycloocta-1,3,6-triene	3.35	−0.10	0.00	50.3	40.2	−112.3	−20.2
3	1,5,9,9-Tetramethyl-2- methylene-spiro [3.5] non-5-ene	1.84	−0.10	0.00	80.6	21.3	−89.3	−17.7
4	Sativan	0.51	−0.41	0.00	42.8	14.1	−80.7	−16.6
5	4,8,8-Trimethyl-2-methylene-4-vinylbicyclo [5.2.0]nonane	2.95	−0.38	0.00	−55.0	1.06	−129.0	−14.9
6	α-Amorphene	3.55	−0.45	0.00	−60.2	1.86	−132.7	−16.5
7	2-Isopropenyl-1,3,5-trimethylbenzene	2.39	−0.45	0.00	−50.3	7.47	−77.5	−16.3
8	α-Gurjunene	3.64	−0.43	0.00	−54.6	4.2	−139	−17.1
9	β-Vatirenene	2.12	−0.23	0.01	−57.6	−3.6	−105	−14.5
10	δ-Cadinene	1.05	−0.41	0.00	−42.0	14.1	−80.7	−16.6
11	β-Guaiene	3.44	−0.76	0.00	−59.2	−2.3	−132.2	−18.2
12	Dehydro-aromadendrene	3.13	−0.20	0.00	−54.3	−3.1	−118.5	−18.0
13	Cubenol	2.96	−0.34	3.26	−422.0	3.32	−66.4	−20.4
14	Ledene	3.34	−0.53	0.00	−56.4	−2.7	−129.8	−17.3
15	Epiglobulol	3.36	−0.04	2.13	35.3	−16.0	−123.5	−18.8
16	Widdrol	3.44	−0.77	1.14	−58.6	−7.3	−132.6	−17.9
17	3-(2-Isopropyl-5-methylphenyl)-2-methylpropionic acid	4.06	−0.87	1.02	−75.5	−7.6	−140.3	−17.1
18	6-Isopropenyl-4,8 a-dimethyl-1,2,3,5,6,7,8,8a-Octahydro-naphthalen-2-ol	3.76	−0.79	1.14	−61.6	3.6	−127.6	−16.8
19	Cedr-8-en-13-ol	4.29	−0.87	1.86	−66.4	−9.0	−139.2	−20.5
20	Isovellerdiol	2.48	−0.31	3.01	−318.6	−22.6	+67.0	−18.2
21	α-Curcumene	1.84	−0.29	0.0	−232.6	41.6	−81.7	−21.1
22	3,3,8,8-Tetramethyl-tricyclo[5.1.0.0(2,4)] oct-5-ene-5-propanoic acid	2.74	−0.22	0.01	33.6	13.4	−128.3	−20.9
23	Solavetivone	2.56	−0.39	3.22	−72.8	−3.73	−52.6	−21.3
24	3,8-Dimethyl-4-(1-methylethylidene)-2,4,6,7,8,8a-Hexahydro-5(1H)-azulenone	3.99	−0.69	1.06	−64.6	−13.7	−145.9	−21.3
25	Spathulenol	3.04	−1.14	0.91	−61.3	0.12	−130.3	−168.8
26	Panduratin[h]	4.11	0.35	1.95	−65.9	−17.5	−118.3	−19.2

[a] Cscore is a consensus scoring which uses multiple types of scoring functions to rank the affinity ofligands

[b] Crash score revealing the inappropriate penetration into the binding site

[c] Polar region of the ligand

[d] Dscore for charge and van der Waals interactions between the protein and the ligand

[e] PMF score indicating the Helmholtz free energies of interactions for protein–ligand atom pairs

[f] Gscore showing hydrogen bonding, complex (ligand–protein), and internal (ligand–ligand) energies

[g] Chemscore points for hydrogen bonding, lipophilic contact, and rotational entropy, along with an intercept term

[h] Reference ligand

Total Energy

Analyzing the total energy is an essential factor to analyze the equilibrium point. The total energy/potential energy/kinetic energy is calculated from short-range Lennard-Jones and short-range Coulomb energies using Gromacs g_energy analysis tool:

$E_{int} = <E_{LJ}> + <E_{Coul}>$ [44].

E_{int} is a crude interaction energy based on short-range energy components. This is not binding energy. This number is a crude qualitative estimate of the stability of enzyme–ligand complex. The energy values obtained for the top ranked complex and the reference complex are shown in revised Fig. 4 and revised Fig. 5, respectively. Ethyl 4-(4-methylphenyl)-4-pentenoate complex has the lowest energy of −540.02 kJ/mol, whereas the reference

Table 3 Binding affinity of active compounds with NS2B–NS3 protease of DENV-2 virus

S.No	Compounds	Cscore[a]	Crash score[b]	Polar score[c]	Dscore[d]	PMF score[e]	Gscore[f]	Chem score[g]
1	Ethyl 4-(4-methylphenyl)-4-pentenoate	5.6	−1.30	0.91	−88.1	18.2	−153.0	−20.8
2	2,3,5,5,8,8-Hexamethyl-cycloocta-1,3,6-triene	3.14	−0.10	0.00	180.1	88.8	−125.2	−21.4
3	1,5,9,9-Tetramethyl-2-methylene-spiro [3.5] non-5-ene	1.61	−0.26	0.00	14.5	67.5	−121.3	−23.3
4	Sativan	2.43	−0.71	0.00	83.6	75.0	−114.0	−19.5
5	4,8,8-Trimethyl-2-methylene-4-vinylbicyclo [5.2.0]nonane	3.75	−1.93	0.00	−83.8	22.8	−194.3	−21.0
6	α-Amorphene	4.51	−1.11	0.00	−85.2	4.14	−195.2	−22.7
7	2-Isopropenyl-1,3,5-trimethylbenzene	4.33	−0.67	0.00	−65.6	15.0	−128.1	−20.1
8	α-Gurjunene	3.38	−0.34	1.25	−58.0	5.54	−120.7	−16.6
9	β-Vatirenene	3.07	0.27	0.01	−45.0	3.3	−110.6	−23.5
10	δ-Cadinene	2.05	−0.31	0.00	−24.0	4.1	−60.7	−16.6
11	β-Guaiene	3.59	−0.41	0.00	−62.3	3.8	−125.7	−19.5
12	Dehydro-aromadendrene	3.19	−0.89	0.00	−70.0	18.9	−140.5	−18.9
13	Cubenol	2.36	−0.76	1.48	−766	58.1	−98.6	−21.6
14	Ledene	2.78	−1.33	0.00	−72.0	23.6	−154.1	−20.0
15	Epiglobulol	5.34	−1.29	4.88	49.6	46.1	−171.9	−22.3
16	Widdrol	2.67	−3.42	0.83	−78.6	31.0	−193.7	−19.6
17	3-(2-Isopropyl-5-methylphenyl)-2-methylpropionic acid	4.12	−1.48	1.12	−88.8	16.3	−186.0	−21.3
18	6-Isopropenyl-4,8 a-dimethyl-1,2,3,5,6,7,8,8a- Octahydro-naphthalen-2-ol	3.95	−0.82	0.88	−74.7	22.9	−120.5	−19.5
19	Cedr-8-en-13-ol	3.36	−1.50	0.00	−72.6	21.3	−175.6	−20.3
20	Isovellerdiol	1.86	−0.53	2.09	−54.5	26.2	−87.4	−18.7
21	α-Curcumene	1.92	−0.72	0.00	−367.6	−0.085	−103.2	−29.7
22	3,3,8,8-Tetramethyl-tricyclo[5.1.0.0(2,4)] oct-5-ene-5-propanoic acid	4.7	−0.10	1.19	119.1	67.8	−131.0	−20.7
23	Solavetivone	1.74	0.34	0.95	−286.3	23.3	−93.3	−25.0
24	3,8-Dimethyl-4-(1-methylethylidene)-2,4,6,7,8,8a-Hexahydro-5(1H)-azulenone	4.01	−0.56	1.34	−66.3	−4.44	−158.7	−21.1
25	Spathulenol	2.23	−1.05	0.00	−64.4	3.14	−144.8	−16.8
26	Panduratin[h]	4.95	−0.69	1.85	−85.2	17.5	−155.3	−19.3

[a] Cscore is a consensus scoring which uses multiple types of scoring functions to rank the affinity of ligands

[b] Crash-score revealing the inappropriate penetration into the binding site

[c] Polar region of the ligand

[d] D-score for charge and van der Waals interactions between the protein and the ligand

[e] PMF-score indicating the Helmholtz free energies of interactions for protein–ligand atom pairs (potential of mean force, PMF)

[f] G-score showing hydrogen bonding, complex (ligand–protein), and internal (ligand–ligand) energies

[g] Chem-score points for hydrogen bonding, lipophilic contact, and rotational entropy, along with an intercept term

[h] Reference ligand

ligand has the value of −523.82 kJ/mol, indicating that interaction with active compound contribute to the more stability of the protein comparing to the reference ligand.

Stability Analysis of Active Compound and Reference Ligand

The RMSD analysis is a key parameter to analyze the equilibration of MD trajectories. RMSD analysis was carried out for the reference ligand and the active compound. Our results show that both the trajectories are well equilibrated. Pictorial representation of RMSD values is illustrated in revised Fig. 6. We observed that both the reference and active compound showed minimum deviation from their starting till 5000 ps. After 5000 ps, the reference complex showed higher deviation than the active complex and attained equilibrium at 0.6 nm at 20,000 ns, whereas active complex attained equilibrium at 0.5 nm at 20,000 ns. Higher RMSD value of reference ligand complex clearly indicated lesser stability of the complex structure than that of the active complex.

Table 4 Binding affinity of active compounds with NS2B–NS3 protease of DENV-3 virus

S.No	Compounds	Cscore[a]	Crash score[b]	Polar score[c]	Dscore[d]	PMF score[e]	Gscore[f]	Chem score[g]
1	Ethyl 4-(4-methylphenyl)-4-pentenoate	5.85	−1.04	1.12	−93.4	21.6	−163.0	−21.4
2	2,3,5,5,8,8-Hexamethyl-cycloocta-1,3,6-triene	3.10	−0.14	0.00	−55.3	51.4	−101.5	−19.3
3	1,5,9,9-Tetramethyl-2- methylene-spiro [3.5] non-5-ene	1.76	−0.06	0.00	50.2	51.4	−104.6	−22.4
4	Sativan	1.23	0.29	0.00	−65.2	−0.23	−77.6	−14.0
5	4,8,8-Trimethyl-2-methylene-4-vinylbicyclo [5.2.0]nonane	3.38	−1.32	0.00	−56.8	−0.90	−154.0	−14.6
6	α-Amorphene	3.30	−0.94	0.00	−59.1	8.02	−133.7	−13.8
7	2-Isopropenyl-1,3,5-trimethylbenzene	2.65	−0.33	0.00	−45.3	5.2	−68.9	−14.3
8	α -Gurjunene	3.29	−0.46	0.00	−47.4	1.29	−134.2	−14.0
9	β-Vatirenene	2.26	−0.21	0.00	−43.2	4.8	−122.5	−13.4
10	δ-Cadinene	1.95	−0.21	0.00	−559	28.4	−85.3	−20.5
11	β-Guaiene	3.60	−0.61	0.00	−53.1	11.2	−124.9	−16.1
12	Dehydro-aromadendrene	2.98	−0.63	0.00	−56.3	10.5	−133.6	−16.5
13	Cubenol	2.88	−0.64	3.18	10.3	−15.3	−65.3	−18.4
14	Ledene	3.34	−0.46	0.00	−56.9	13.3	−133.3	−16.4
15	Epiglobulol	5.45	0.26	4.57	39.5	29.9	−118.0	−22.0
16	Widdrol	3.5	−0.47	2.08	−51.7	7.3	−116.6	−18.7
17	3-(2-Isopropyl-5-methylphenyl)-2-methylpropionic acid	3.80	−0.77	2.49	−57.5	11.2	−94.0	−14.5
18	6-Isopropenyl-4,8 a-dimethyl-1,2,3,5,6,7,8,8a- Octahydro-naphthalen-2-ol	4.72	−0.59	2.44	−49.5	5.4	−104.4	−16.9
19	Cedr-8-en-13-ol	3.17	−1.40	2.12	−60.4	14.7	−138.8	−19.9
20	Isovellerdiol	2.20	−1.30	1.96	12.0	44.2	−112.2	−21.5
21	α-Curcumene	1.73	−0.45	0.00	−704	27.2	−73.9	−17.7
22	3,3,8,8-Tetramethyl-tricyclo[5.1.0.0(2,4)] oct-5-ene-5-propanoic acid	3.34	−0.199	1.04	49.5	33.1	−108.9	−16.4
23	Solavetivone	1.77	−0.53	1.76	−588.8	21.7	−67.4	−20.3
24	3,8-Dimethyl-4-(1-methylethylidene)-2,4,6,7,8,8a-Hexahydro-5(1H)-azulenone	3.31	−0.61	1.14	−46.4	−2.9	−118.7	−17.2
25	Spathulenol	2.66	−0.31	1.06	−47.1	7.7	−104.3	−14.3
26	Panduratin[h]	4.95	−0.85	1.05	−85.2	16.2	150.1	−19.8

[a] Cscore is a consensus scoring which uses multiple types of scoring functions to rank the affinity of ligands

[b] Crash score revealing the inappropriate penetration into the binding site

[c] Polar region of the ligand

[d] Dscore for charge and van der Waals interactions between the protein and the ligand

[e] PMF score indicating the Helmholtz free energies of interactions for protein–ligand atom pairs

[f] Gscore showing hydrogen bonding, complex (ligand–protein), and internal (ligand–ligand) energies

[g] Chemscore points for hydrogen bonding, lipophilic contact, and rotational entropy, along with an intercept term

[h] Reference ligand

Root Mean Square Fluctuation

Differences in flexibility among the residues were analyzed using the parameter root mean square deviation. RMSF values of the backbone atoms of each residue in DENV-4–Ethyl 4-(4-methylphenyl)-4-pentenoate complex and DENV-4–panduratin complex were calculated, and the results are shown in revised Fig. 7. From the figure, it can be observed that DENV-4–Ethyl 4-(4-methylphenyl)-4-pentenoate show less fluctuation than DENV-4–panduratin complex indicating the restricted movements during simulation.

H-Bond Analysis

Hydrogen bond plays a crucial role in the overall stability of the protein structure. Intermolecular hydrogen bonds were analyzed for the reference ligand as well as for the

Table 5 Binding affinity of active compounds with NS2B–NS3 protease of DENV-4 virus

S.No	Compounds	Cscore[a]	Crash score[b]	Polar score[c]	Dscore[d]	PMF score[e]	Gscore[f]	Chem score[g]
1	Ethyl 4-(4-methylphenyl)-4-pentenoate	6.32	−1.42	2.38	−94.71	−28.6	−144	−24.8
2	2,3,5,5,8,8-Hexamethyl-cycloocta-1,3,6-triene	4.58	−0.14	0.00	241	28.9	−129.6	−20.6
3	1,5,9,9-Tetramethyl-2- methylene-spiro [3.5] non-5-ene	2.21	−0.13	0.00	23.6	14.6	−108.4	−19.4
4	Sativan	1.28	−0.53	0.00	10.5	10.1	−90.7	−19.6
5	4,8,8-Trimethyl-2-methylene-4-vinylbicyclo [5.2.0]nonane	4.67	−0.63	0.00	−75.9	−6.4	−165.7	−19.7
6	α-Amorphene	5.28	−0.83	1.05	−80	−30.3	−179.6	−22.4
7	2-Isopropenyl-1,3,5-trimethylbenzene	3.05	−0.56	0.00	−62.6	1.4	−112.4	−20.0
8	α -Gurjunene	4.64	−0.34	0.00	−71.3	−24.5	−156.8	−19.9
9	β-Vatirenene	2.13	−0.23	0.01	−45.8	−2.06	−105.4	−17.5
10	δ-Cadinene	1.33	−0.35	0.00	−359.5	−16.5	−75.8	−21.7
11	β-Guaiene	2.99	−0.40	0.00	−59.1	−1.05	−111.6	−19.2
12	Dehydro-aromadendrene	4.49	−0.45	0.00	−77.1	−22.3	−157.5	−20.2
13	Cubenol	1.55	−1.14	0.00	−98.2	−28.0	−116.3	−19.1
14	Ledene	4.06	−0.54	0.00	−73.1	−19.2	−147.7	−20.7
15	Epiglobulol	3.97	−0.80	2.91	−72.1	−11.8	−146.6	−19.5
16	Widdrol	5.4	−0.83	1.05	−80	−30.3	−179.6	−22.4
17	3-(2-Isopropyl-5-methylphenyl)-2-methylpropionic acid	4.89	−0.62	1.01	−77.6	−39.9	−156.2	−16.3
18	6-Isopropenyl-4,8 a-dimethyl-1,2,3,5,6,7,8,8a- Octahydro-naphthalen-2-ol	4.77	−0.63	0.00	−83.3	−33.9	−165.7	−16.6
19	Cedr-8-en-13-ol	4.83	−1.00	1.10	−82.6	−39.36	−166.8	−18.9
20	Isovellerdiol	3.34	−0.54	3.00	−817	−26.8	−102.1	−25.2
21	α-Curcumene	2.57	−0.46	0.00	−524.9	16	−105.5	−23.6
22	3,3,8,8-Tetramethyl-tricyclo[5.1.0.0(2,4)] oct-5-ene-5-propanoic acid	4.47	−0.19	0.00	188	6.84	−146.3	−19.1
23	Solavetivone	1.50	−0.48	1.74	−313.6	17.5	−72.7	−23.4
24	3,8-Dimethyl-4-(1-methylethylidene)-2,4,6,7,8,8a-Hexahydro-5(1H)-azulenone	3.09	−1.02	0.06	−65.6	1.6	−136.7	−17.7
25	Spathulenol	4.82	−0.94	0.91	−81.3	−52.4	−193.5	−21.4
26	Panduratin[h]	6.02	−1.05	2.11	−90.1	−19.5	−135	−23.1

[a] Cscore is a consensus scoring which uses multiple types of scoring functions to rank the affinity of ligands

[b] Crash score revealing the inappropriate penetration into the binding site

[c] Polar region of the ligand

[d] Dscore for charge and van der Waals interactions between the protein and the ligand

[e] PMF score indicating the Helmholtz free energies of interactions for protein–ligand atom pairs

[f] Gscore showing hydrogen bonding, complex (ligand–protein), and internal (ligand–ligand) energies

[g] Chemscore points for hydrogen bonding, lipophilic contact, and rotational entropy, along with an intercept term

[h] Reference ligand

active compound, and the results are shown in revised Fig. 8 and revised Fig. 9. Our analysis illustrated that both the complexes showed three intermolecular hydrogen bonds throughout the simulation. Even though reference ligand showed three hydrogen bonds, the number of stable hydrogen bonds was comparatively lesser. Based on the hydrogen bond analysis, we observed that the active compound Ethyl 4-(4-methylphenyl)-4-pentenoate–DENV-4 complex contributed more stability to the enzyme–ligand complex compared to the reference ligand panduratin. Further the hydrogen and hydrophobic interactions between the active compound and DENV-4 is illustrated in revised Fig. 10.

Drug-likeness and Molecular Properties of Active Compounds

Natural products are commonly considered as a rich source of biologically active substances. Many drugs approved by Food and Drug Administration (FDA)

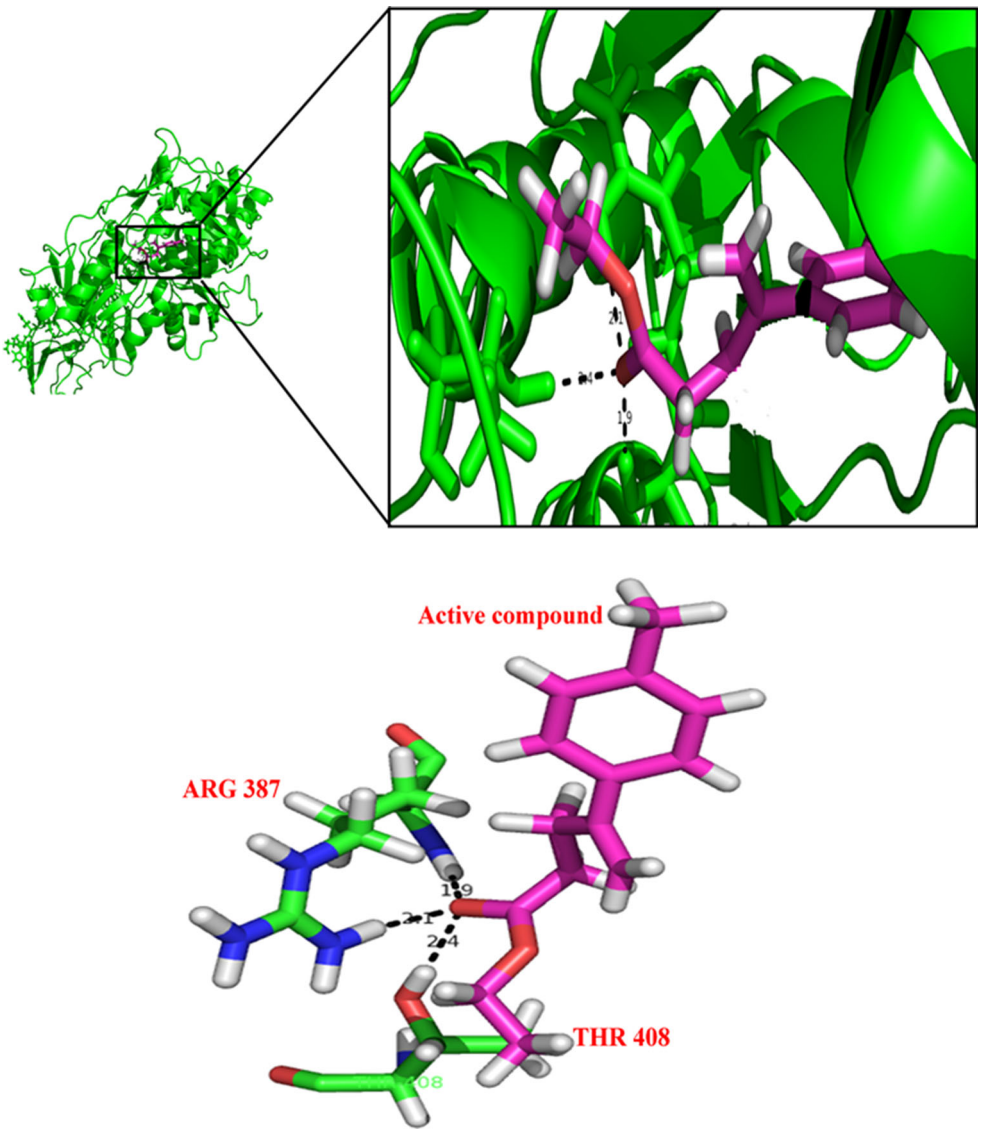

Fig. 2 *Pictorial* representation hydrogen bond interactions between the active compound Ethyl 4-(4-methylphenyl)-4-pentenoate and the active site residues of DENV-4. *Dotted lines* represent the hydrogen bonds interactions between H atom of Thr 408 with O atom of active compound, H atom of Arg 387 with O atom of Arg 387 with O atom of active compound

directly come from natural products. Approximately 60 % of cancer drugs and 75 % of infectious disease drugs are derived from natural products [45]. The pharmacokinetic properties of the compound Ethyl 4-(4-methylphenyl)-4-pentenoate which showed maximum binding affinity with the NS2B–NS3 protease of dengue virus were analyzed based on "Lipinski's rule of five" and results are given in revised Table 7. Lajiness and colleagues proposed that a compound is considered to be oral dug when it possesses a structure which shows favorable interaction with the receptor [46]. Our result shows that the compound Ethyl 4-(4-methylphenyl)-4-pentenoate successfully passed through the ADME filter without any violation. Further ADME profiling of the active compound Ethyl 4-(4-methylphenyl)-4-pentenoate was analyzed for the essential parameters, and the results are presented in revised Table 8. Recently, it has been reported that 98 % of drugs fail in clinical trials due to poor blood–brain barrier (BBB) [47, Geldenshuys]. As the name implies, blood–brain barrier separates brain and central nervous system (CNS) from the bloodstream [48]. P-glycoprotein receptor plays an important role in transporting the drug across the blood–brain barrier and intestinal epithelial cells. Various neurological complications such as meningoencephalitis, encephalopathy, and encephalitis are also reported to be associated with dengue virus infections [49]. Therefore, our compound should pass through the BBB barrier in order to exhibit CNS activity. Our analysis on BBB permeability showed positive results indicating the ability of the active compound to pass through the BBB barrier. Caco-2 permeability plays a crucial role in drug

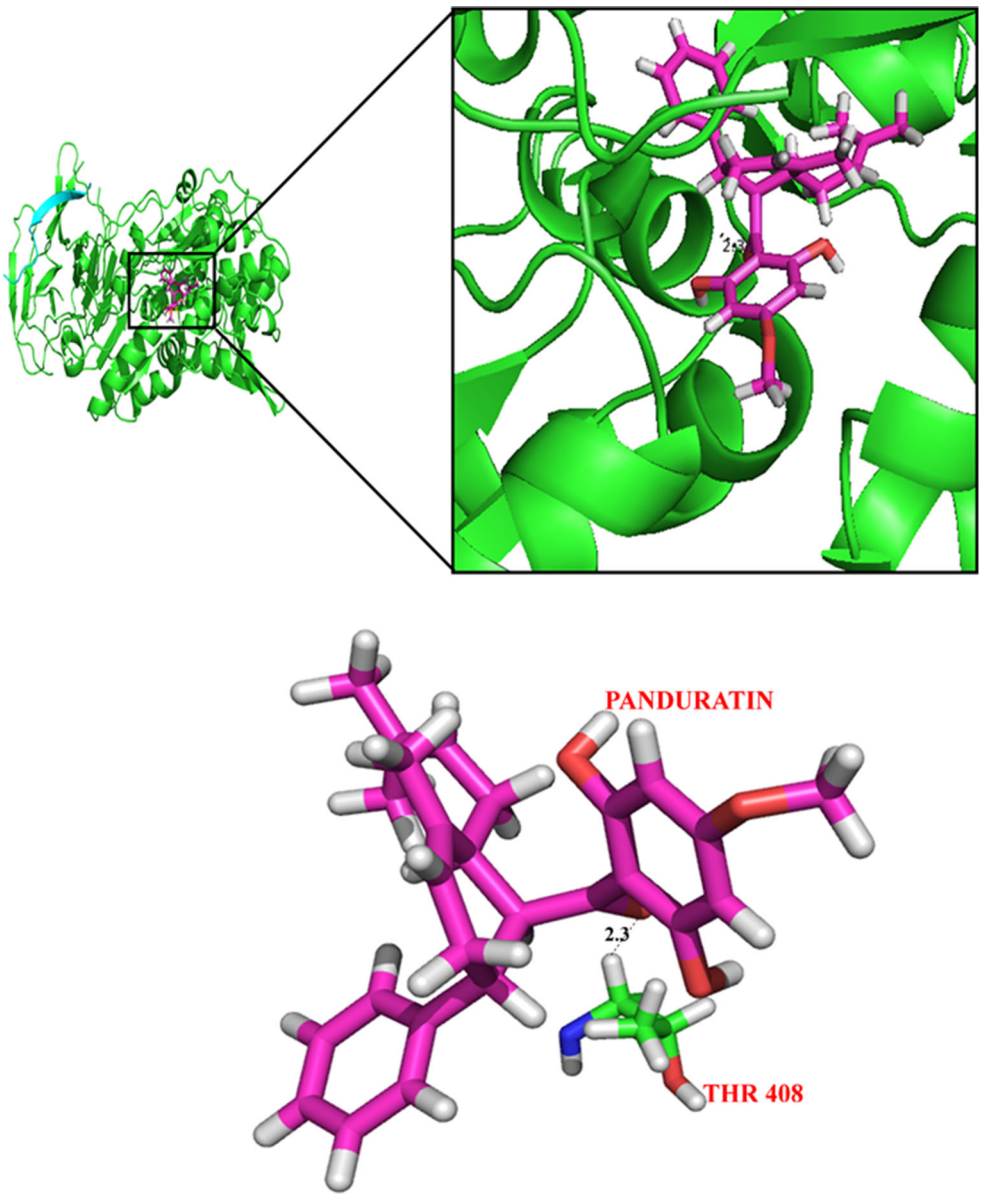

Fig. 3 *Pictorial* representation hydrogen bond interactions between the reference ligand panduratin and the active site residues of DENV-4. *Dotted lines* represent the hydrogen bonds interactions between H atom of Thr 408 with O atom of active compound

discovery process as it exhibits morphological as well as functional similarities with the human intestinal enterocytes. These cells express a variety of transport systems, including Pgp of efflux proteins and also other dipeptide transporters (PEPT1) that are commonly found in small intestinal enterocytes [50]. Since it possesses the expression of multiple transport systems, it has got a greater advantage over simplified models. ADME profiling of Ethyl 4-(4-methylphenyl)-4-pentenoate on Caco-2 permeability showed good correlation with human intestinal absorption. Cytochrome p450 comprised the major portion of the enzymes in phase I which included oxidation, reduction, and hydrolysis. Even though more than 50 CYPs have been identified, CYP3A subfamily represents the major component of a phase I metabolism. CYP3A is responsible for metabolizing nearly half of the marketed xenobiotics, environmental carcinogens, and other endogenous compounds like steroids [51]. Analyzing the intestinal epithelial permeability is an important criterion to determine the rate and extent of drug absorption. Compounds with poor permeability show poor in vivo absorption [52]. Our compound Ethyl 4-(4-methylphenyl)-4-pentenoate showed positive value in Human Intestinal Absorption (HIA) absorption confirming the capability of the compound to pass through the intestinal epithelial barrier. In conclusion, ADME

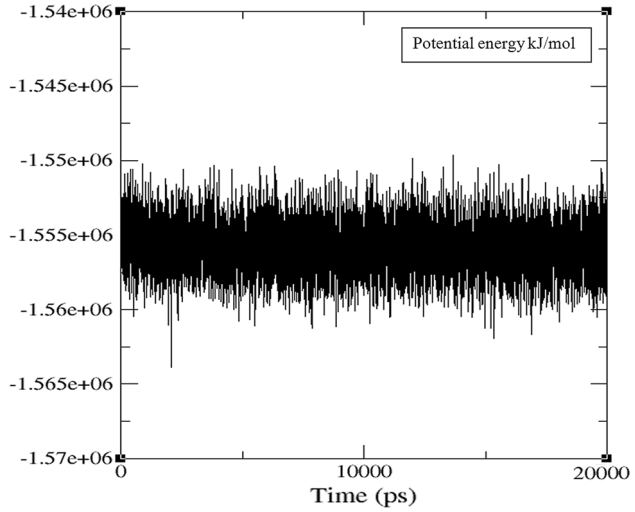

Fig. 4 Time dependence of total energy for DENV-4–Ethyl 4-(4-methylphenyl)-4-pentenoate complex (kJ/mol)

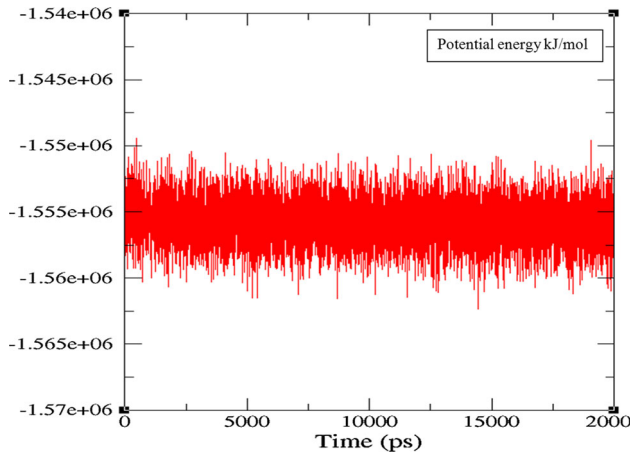

Fig. 5 Time dependence of total energy for DENV-4–panduratin complex

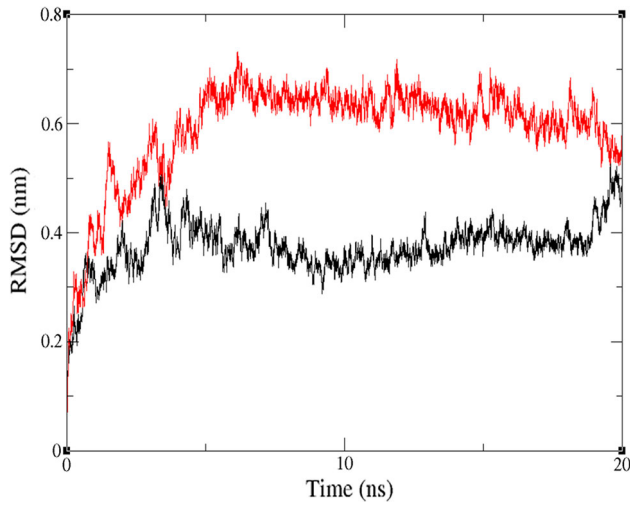

Fig. 6 Root mean square deviations correspond to MD simulation at 300 k. *Black color* indicates Ethyl 4-(4-methylphenyl)-4-pentenoate–protease complex; *red color* indicates panduratin–protease complex (Color figure online)

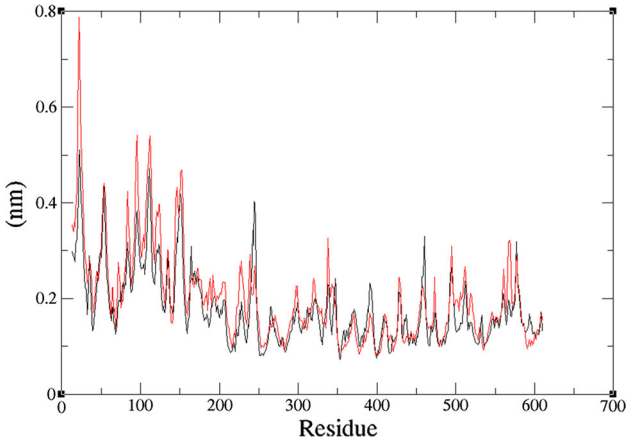

Fig. 7 Root mean square fluctuation corresponds to MD simulation at 300 k. *Black color* indicates Ethyl 4-(4-methylphenyl)-4-pentenoate–DENV-4 complex; *red color* indicates panduratin complex (Color figure online)

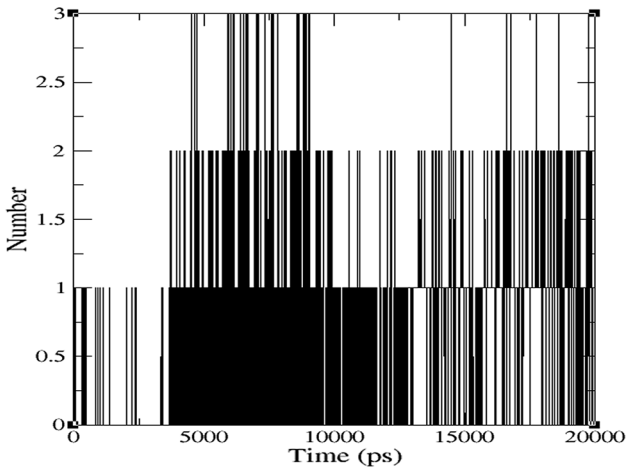

Fig. 8 H bonds observed between the active compound Ethyl 4-(4-methylphenyl)-4-pentenoate and DENV-4 protease along the MD simulation

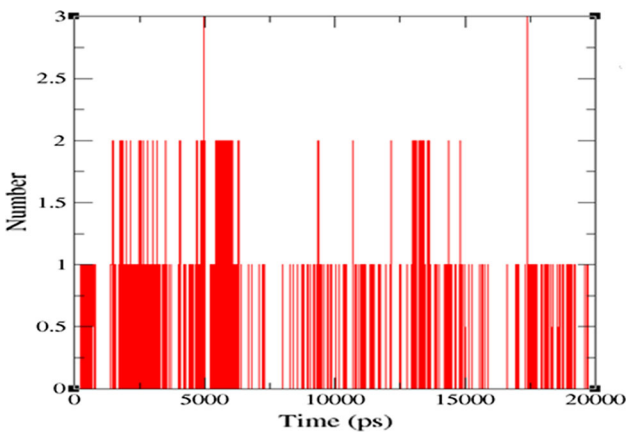

Fig. 9 H bonds observed between the reference ligand panduratin and DENV-4 protease along the MD simulation

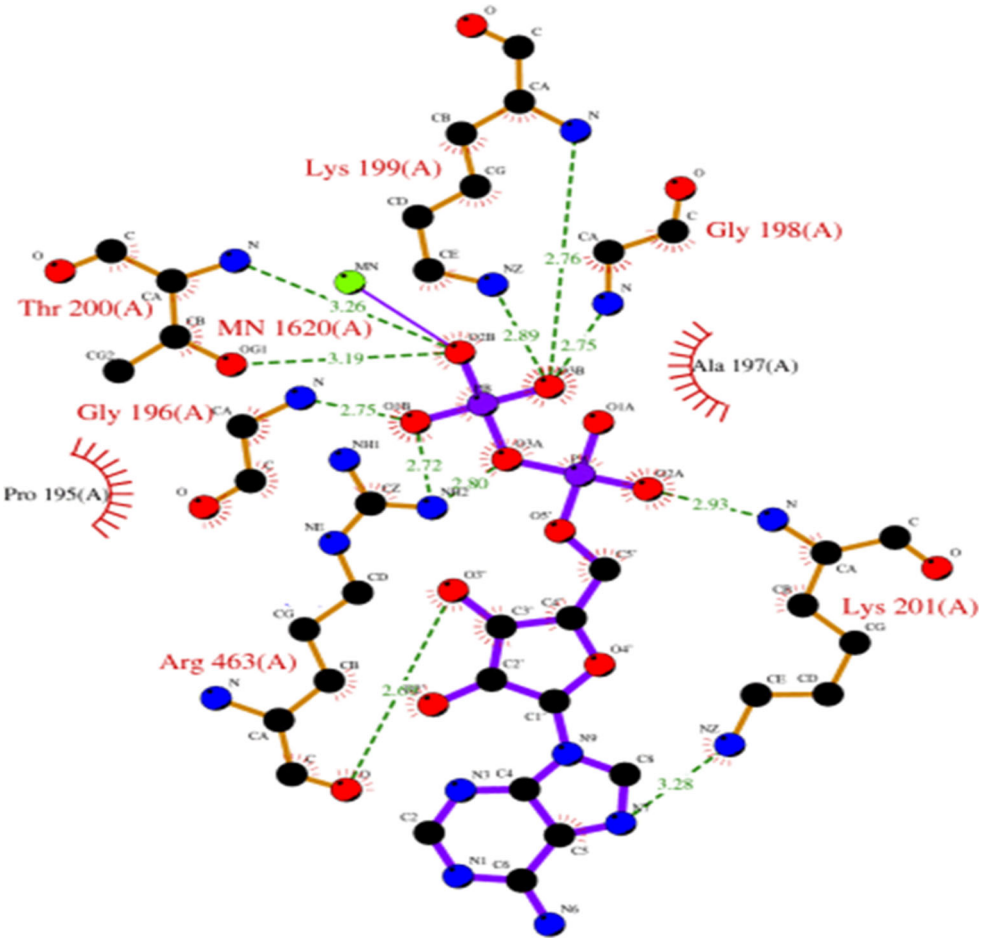

Fig. 10 Hydrogen and hydrophobic interactions between the top scored active compound and DENV-4 protease. Hydrogen bonds are indicated by *dashed green lines* (with the distance between acceptor and donor atoms) and the hydrophobic contacts are represented by *an arc* (Color figure online)

Table 6 Comparison of binding energy for the active compound Ethyl 4-(4-methylphenyl)-4-pentenoate and the reference ligand panduratin

Conformations	Active compound–DENV-4 (kcal/mol)	Panduratin–DENV-4 (kcal/mol)
1	−6.35	−6.25
2	−5.93	−5.84
3	−5.86	−5.75
4	−4.75	−4.05
5	−5.35	−5.20
6	−3.75	−3.25
7	−4.72	−4.13
8	−5.99	−3.07
9	−4.81	−3.97
10	−4.93	−4.75
11	−3.46	−3.23

profiling of Ethyl 4-(4-methylphenyl)-4-pentenoate fulfilled all the criteria necessary to act as a drug. Our results indicate that among the 25 compounds screened,

Table 7 Molecular properties and drug-likeness of Ethyl 4-(4-methylphenyl)-4-pentenoate

Compound	Ethyl 4-(4-methylphenyl)-4-pentenoate
PubChem CID	589,505
Molecular weight	218
LogP (octanol–water partition coefficient value)	3.8
H-bond donor	0
H-bond acceptor	2

the compound Ethyl 4-(4-methylphenyl)-4-pentenoate showed prospective antiviral activity against dengue virus protease. Further, the positive results observed in molecular properties and drug-likeness of the Ethyl 4-(4-methylphenyl)-4-pentenoate endorsed the capability of the compound to be developed as a drug. Our results strongly suggest that Ethyl 4-(4-methylphenyl)-4-pentenoate is a good candidate for the development of an effective antidengue compound.

Table 8 ADMET predicted profile for the active compound Ethyl 4-(4-methylphenyl)-4-pentenoate

(a) Absorption	
Models	
Blood–brain barrier	BBB+
Human intestinal absorption	HIA+
Caco-2 permeability	Caco2+
P-glycoprotein Inhibitor	NI
Renal organic cation transporter	NI
(b) Metabolism	
CYP450 2C9 substrate	NS
CYP450 2D6 substrate	NS
CYP450 3A4 substrate	NS
CYP450 1A2 inhibitor	NI
CYP450 2C9 inhibitor	NI
CYP450 2D6 inhibitor	NI
CYP450 2C19 inhibitor	NI
CYP450 3A4 inhibitor	NI
(c) Toxicity	
AMES toxicity	NT
Carcinogens	NC

NI noninhibitor, *NS* nonsubstrate, *NT* nontoxic, *NC* noncarcinogen

Acknowledgments Dr. Anand Anbarasu and Dr. Sudha Ramaiah gratefully acknowledge the Indian Council of Medical Research (ICMR), Government of India Agency for the research grant [IRIS ID: 2014-0099]. P. Lavanya thanks ICMR for the Research fellowship. We would like to thank the management of VIT University for providing us the necessary facilities to carry out this research project.

Compliance with Ethical Standards

Conflict of Interest The authors declare that there is no conflict of interest.

References

1. Hynes, N. A. (2012). Dengue: A reemerging concern for travelers. *Cleveland Clinic Journal of Medicine, 9*, 7474–7482.
2. Tomlinson, S. M., & Watowich, S. J. (2011). Anthracene-based inhibitors of dengue virus NS2B–NS3 protease. *Antiviral Research, 89*, 127–135.
3. Wang, Q. Y., Patel, S. J., Vangrevelinghe, E., Xu, H. Y., Rao, R., Jaber, D., et al. (2009). A small-molecule Dengue virus entry inhibitor. *Antimicrobial Agents and Chemotherapy, 53*, 51823–51831.
4. Qing, M., Zou, G., Wang, Q. Y., Xu, H. Y., Dong, H., Yuan, Z., & Shi, P. Y. (2010). Characterization of Dengue virus resistance to Brequinar in cell culture. *Antimicrobial Agents and Chemotherapy, 54*, 3686–3695.
5. Gromowski, G. D., Barrett, N. D., & Barrett, A. D. T. (2008). Characterization of Dengue virus complex-specific neutralizing epitopes on envelope protein domain III of Dengue 2 virus. *Journal of Virology, 82*, 8828–8837.
6. Luo, D., Xu, T., Hunke, C., Gruber, G., Vasudevan, S. G., & Lescar, J. (2008). Crystal structure of N3 protease—helicase from dengue virus. *Journal of Virology, 82*, 173–183.
7. Wang, Q. Y., Kondreddi, R. R., Xie, X., Rao, R., Nilar, S., Xu, H. Y., et al. (2011). A translation inhibitor that suppresses Dengue virus in vitro and in vivo. *Antimicrobial Agents and Chemotherapy, 55*, 4072–4080.
8. Falgout, B., Pethel, M., Zhang, Y. M., & Lai, C. J. (1991). Both nonstructural proteins NS2B and NS3 are required for the proteolytic processing of Dengue virus nonstructural proteins. *Journal of Virology, 65*, 2467–2475.
9. Chambers, T. J., Nestorowicz, A., Amberg, S. M., & Rice, C. M. (1993). Mutagenesis of the yellow fever virus NS2B protein: effects on proteolytic processing, NS2B–NS3 complex formation, and viral replication. *Journal of Virology, 67*, 6797–6807.
10. Wu, C. F., Wang, S. H., Sun, C. M., Hu, S. T., & Syu, W. J. (2003). Activation of dengue protease autocleavage at the NS2B–NS3 junction by recombinant NS3 and GST-NS2B fusion proteins. *Journal of Virological Methods, 114*, 45–54.
11. Tomlinson, S. M., Malmstrom, R. D., Russo, A., Mueller, N., Pang, Y. P., & Watowich, S. J. (2009). Structure-based discovery of dengue virus protease inhibitors. *Antiviral Research, 82*, 110–114.
12. Rates, S. M. K. (2001). Plants as source of drugs. *Toxicon, 39*, 603–613.
13. Lanini, J., Almeida, J. M. D., Nappo, S. A., & Carlini, E. A. (2012). Are medicinal herbs safe? The opinion of plant vendors from Diadema (Sao Paulo, southeastern Brazil). *Revista Brasileira de Farmacognosia, 22*, 21–28.
14. Kim, H., Chen, F., Wang, X., Chung, H. Y., & Jin, Z. (2005). Evaluation of antioxidant activity of vetiver (*Vetiveria zizanioides* L) oil and identification of its antioxidant activity constituents. *Journal of Agriculture and Food Chemistry, 53*, 7691–7695.
15. Singh, S. P., Sharma, S. K., Singh, T., & Singh, L. (2013). Review on Vetiveria zizanioides: A medicinal herb. *JDDT, 1*, 80–83.
16. Peng, H. Y., Lai, C. C., Lin, C. C., & Chou, S. T. (2014). Effect of *Vetiveria zizanioides* essential oil on melanogenesis in melanoma cells: Downregulation of tyrosinase expression and suppression of oxidative stress. *The Scientific World Journal*. doi:10.1155/2014/213013.
17. Maffei, M. (2002). *Vetiveria: The genus vetiveria* (p. 73). Boca Raton: CRC Press.
18. Berman, H. M., Westbrook, J., Feng, Z., Gilliland, G., Bhat, T. N., Weissig, H., et al. (2000). The protein data bank. *Nucleic Acid Research, 28*, 235–242.
19. Chandramouli, S., Joseph, J. S., Daudenarde, S., Gatchalian, J., Ty, C. C., & Kuhn, P. (2010). Serotype-Specific structural differences in the protease-cofactor complexes of the dengue virus family. *Journal of Virology, 84*, 3059–3067.
20. Erbel, P., Schiering, N., D'Arch, A., Renatus, M., Kroemer, M., Lim, S. P., et al. (2006). Structural basis for the activation of flaviviral NS3 proteases from dengue and West Nile virus. *Nature Structural & Molecular Biology, 13*, 372–373.
21. Noble, C. G., She, C. C., Chao, A. T., & Shi, P. Y. (2012). Ligand-bound structures of the dengue virus protease reveal the active conformation. *Journal of Virology, 86*, 438–446.
22. Luo, D., Wei, N., Daon, D. N., Paradkar, P. N., Chong, Y., Davidson, A. D., et al. (2010). Flexibility between the protease and helicase domains of the dengue virus NS3 protein conferred by the linker region and its functional implications. *Journal of Biological Chemistry, 285*, 18817–18827.
23. Chou, S. T., Lai, C. P., Lin, C. C., & Shih, Y. (2012). Study of the chemical composition, antioxidant activity and anti-inflammatory activity of essential oil from *Vetiveria zizanioides*. *Food Chemistry, 134*, 262–268.
24. Frimayanthi, N., Chee, C. F., Zain, S. M., & Rahman, N. A. (2011). Design of new competitive Dengue Ns2b/Ns3 protease

inhibitors—a computational approach. *International Journal of Molecular Sciences, 12*, 1089–1100.
25. Jain, A. N. (2003). Surflex: fully automatic flexible molecular docking using a molecular similarity-based search engine. *Journal of Medicinal Chemistry, 46*, 499–511.
26. Jones, G., Willett, P., & Glen, R. C. (1995). Molecular recognition of receptor sites using a genetic algorithm with a description of desolvation. *Journal of Molecular Biology, 245*, 43–53.
27. Meng, E. C., Shoichet, B. K., & Kuntz, I. D. (1992). Automated docking with grid-based energy evaluation. *Journal of Computational Chemistry, 13*, 505–524.
28. Eldridge, M. D., Murray, C. W., Auton, T. R., Paolini, G. V., & Mee, R. P. (1997). Empirical scoring functions: I. The development of a fast empirical scoring function to estimate the binding affinity of ligands in receptor complexes. *Journal of Computer-Aided Molecular Design, 11*, 425–445.
29. Ling, B., Bi, S., Sun, M., Jing, Z., Li, X., & Zhang, R. (2014). Molecular dynamics simulations of mutated *Mycobacterium tuberculosis* L-alanine dehydrogenase to illuminate the role of key residues. *Journal of Molecular Graphics and Modelling, 50*, 61–70.
30. Hess, B., Kutzner, C., Spoel, D. V. D., & Lindahl, E. (2008). GROMACS 4: Algorithms for highly efficient, load-balanced, and Scalable molecular simulation. *Journal of Chemical Theory and Computation, 4*, 435–447.
31. Lee, H. C., Hsu, W. C., Liu, A. L., Hsu, C. J., & Sun, Y. C. (2014). Using thermodynamic integration MD simulation to compute relative protein-ligand binding free energy of a GSK3β kinase inhibitor and its analogs. *Journal of Molecular Graphics and Modelling, 51*, 37–49.
32. Suhre, K., & Sanejouand, Y. H. (2015). ElNemo: a normal mode web server for protein movement analysis and the generation of templates for molecular replacement. *The Journal of Physical Chemistry B, 119*, 15395–15406.
33. Spoel, D. V. D., Lindahl, E., Hess, B., & Groenhof, G. (2005). GROMACS: Fast, flexible and free. *Journal of Computational Chemistry, 26*, 1707–1718.
34. Cheng, F., Li, W., Zhou, Y., Shen, J., Wu, Z., Liu, G., et al. (2012). admetSAR: A comprehensive source and free tool for evaluating chemical ADMET properties. *Journal of Chemical Information and Modeling, 52*, 3099–3105.
35. Lavanya, P., Ramaiah, S., & Anbarasu, A. (2015). Computational analysis reveal inhibitory action of nimbin against dengue viral envelope protein. *Virus Disease, 26*, 243–254.
36. Hao, G. F., Yang, G. F., & Zhan, C. G. (2012). Structure-based methods for predicting target mutation-induced drug resistance and rational drug design to overcome the problem. *Drug Discovery Today, 17*, 1121–1126.
37. Badia, E., Oliva, J., Balaguer, P., & Cavailles, V. (2007). Tamoxifen resistance and epigenetic modifications in breast cancer cell lines. *Current Medicinal Chemistry, 14*, 3035–3045.
38. Jenwitheesuk, E., & Samudrala, R. (2005). Prediction of HIV-1 protease inhibitor resistance using a protein-inhibitor flexible docking approach. *Antiviral Therapy, 10*, 157–166.
39. Layten, M., Hornak, V., & Simmerling, C. (2006). The open structure of a multi-drug-resistant HIV-1 protease is stabilized by crystal packing contacts. *Journal of the American Chemical Society, 128*, 13360–13361.
40. Moreira, I. S., Fernandes, P. A., & Ramos, M. J. (2007). Computational alanine scanning mutagenesis-an improved methodological approach. *Journal of Computational Chemistry, 28*, 644–654.
41. Senthilvel, P., Lavanya, P., Kumar, K. M., Swetha, R., Anitha, P., Bag, S., et al. (2013). Flavonoid from Carica papaya inhibits NS2B–NS3 protease and prevents Dengue 2 viral assembly. *Bioinformation, 9*, 18.
42. Tomlinson, S. M., Malmstrom, R. D., & Watowich, S. J. (2011). New approaches to structure-based discovery of dengue protease inhibitors. *Infectious Disorders-Drug Targets, 9*, 327–343.
43. Xie, X., Zou, J., Wang, Q. Y., Noble, C. G., Lescar, J., & Shi, P. Y. (2005). Generation and characterization of mouse monoclonal antibodies against NS4B protein of dengue virus. *Virology, 450*, 250–257.
44. Mishra, N. K., Deepak, R. N. V. K., Sankararamakrishnan, R., & Verma, S. (2015). Controlling in vitro insulin amyloidosis with stable peptide conjugates: A combined experimental and computational study. *Journal of Physical Chemistry B, 119*, 15395–15406.
45. Zhang, L., & Demain, A. L. (2005). *Natural products: Drug discovery and therapeutic medicine*. New York: Humana Press.
46. Lajiness, M. S., Vieth, M., & Erickson, J. (2004). Molecular properties that influence oral drug-like behavior. *Current Opinion in Drug Discovery and Development, 7*, 470–477.
47. Geldenshuys, W. J., Allen, D. D., & Bloomquist, J. R. (2012). Novel models for assessing blood–brain barrier drug permeation. *Expert Opinion on Drug Metabolism & Toxicology, 8*, 647653.
48. Alavijeh, M. S., Chishty, M., Qaiser, Z. M., & Palmr, A. M. (2005). Drug metabolism and pharmacokinetics, the blood–brain barrier, and central nervous system drug discovery. *NeuroRx, 2*, 554–571.
49. Artal, C. F. J., Wichmann, O., Farrar, J., & Gascon, J. (2013). Neurological complications of dengue virus infection. *The Lancet Neurology, 12*, 906–919.
50. Bohets, H., Annaert, P., Mannes, G., Beijsterveldt, L. V., Anciaux, K., Verboven, P., et al. (2001). Strategies for absorption screening in drug discovery and development. *Current Topics in Medicinal Chemistry, 1*, 367–383.
51. Bezirtzoglou, E. E. V. (2012). Intestinal chromosomes P450 regulating the intestinal microbiota and its probiotic profile. *Microbial Ecology in Health and Disease*. doi:10.3402/mehd.v23i0.18370.
52. Wessel, M. D., Jurs, P. C., Tolan, J. W., & Muskal, S. M. (1998). Prediction of human intestinal absorption of drug compounds from molecular structure. *Journal of Chemical Information and Computer Sciences, 38*, 726–735.